Performance of Steel Grain Silos and Rural Communities to Windstorms

Lianne Brito[1] and Christine Wittich, Ph.D., A.M.ASCE[2]

[1]Undergraduate Student, Dept. of Civil, Environmental, and Construction Engineering, Univ. of Central Florida, Orlando, FL 32816-2450. E-mail: lianne.brito@knights.ucf.edu
[2]Assistant Professor, Dept. of Civil Engineering, Univ. of Nebraska–Lincoln, Lincoln, NE 68588-6105. E-mail: cwittich@unl.edu

ABSTRACT

Rural communities are home to millions of people and small businesses, and are found in a wide range of geographic locations across the United States. As such, these rural areas are routinely subjected to extreme loads and natural hazards including earthquakes, tornadoes, and hurricanes. It is an enormous challenge to quantify the scale and extent of natural hazards' damage on rural communities, particularly when considering the various components such as destroyed feed supplies, livestock losses, damage to barns and other structures, etc. This challenge is exacerbated by the lack of knowledge regarding the response of many rural systems to weather and climate disasters. Therefore, as a first step towards understanding the impacts of natural hazards on rural communities, this paper first presents the results of a digital/virtual reconnaissance of rural communities that have been subjected to a natural hazard during the first seven months of 2018. The results of this digital reconnaissance, in combination with traditional reconnaissance, highlighted that large steel grain silo structure is particularly susceptible to windstorms. To gain further insight into this problem, a numerical model of this structure in LS-DYNA is presented and used within a parametric study to identify the key geometric and load properties that lead to failure of the structure.

INTRODUCTION

Enhancing the resilience of our communities and the infrastructure that support them has been identified as a national imperative. The National Research Council defines resilience as "the ability to prepare and plan for, absorb, recover from, and more successfully adapt to adverse event" (NRC 2012). While extensive research has been conducted on urban vulnerability and resilience, there has been considerably less on rural resilience (e.g., Cutter, Ash, and Emrich, 2016). Despite this lack of attention, the US agricultural industry suffered losses in excess of 5 billion dollars in 2017 alone (Bloch, 2018). In this context, rural areas cover 97 percent of the nation's land area and include 60 million people, representing 19.3 percent of the United States population (New Census Data, 2016). Due to the geographic spread and relatively low population density, it is an enormous challenge to quantify the scale and extent of natural hazards' damage on rural communities, especially when considering the various economic and infrastructure sectors that can be damaged including feed supplies, livestock losses, structural damage to barns, storehouses, or transportation routes, etc. While many government agencies, such as the Federal Emergency Management Agency (FEMA) and the National Oceanic and Atmospheric Administration (NOAA), provide digital information about the impact of natural disasters around the United States, a focused study or reconnaissance effort of rural communities that have undergone a natural hazard has not been conducted to the authors' knowledge. The extensive losses that can result due to natural hazards in rural areas affect the long-term resilience as well as the sustainability of the communities affected, making it more difficult for

the present need of accessible health care, goods and other services. (Cutter, Ash, and Emrich, 2016). Therefore, there is a critical need to quantifiably assess the performance of rural communities to natural hazards and identify those systems that contribute to their low resilience.

A uniquely rural infrastructure system that is highly vulnerable to extreme loads and tends to perform poorly in most natural hazards (earthquakes, tornadoes/windstorms, hurricanes, etc.) is the large grain silo structure – see Figures 1 and 2. While these silos can be constructed of many materials and encompass a wide range of geometric configurations, they are typically a thin-walled steel cylindrical structure with a conical or dome roof. Throughout the years, more refined distinctions have been created between silo structures and bins, as shown in Figure 1, where bins or bunkers are usually shallow structures containing coal, coke, ore, crushed stone, gravel, and similar materials; and, silo structures are taller structures containing materials such as grain and cement (Li, 1994).

A similar system that is susceptible to natural disasters is the aboveground storage tank (AST), as shown in Figure 1c, which is a similarly a large cylindrical structure with a thin metal wall, typically used to store hazardous substances such as oil (e.g., Kameshwar, 2018). While ASTs and concrete silos are designed according to the American Petroleum Institute and the American Concrete Institute, respectively, there is no one mandated code or general design philosophy for these critical agricultural storage structures (Dogangun et al., 2009). Given this lack of consistency in design, the performance of these structures under extreme loads is largely uncertain. However, silos have been observed to fail with a much higher frequency than other industrial structures both in response to various natural hazards as well as during routine use (Dogangun et. al, 2009). Even though the failure of silo structures does not typically lead to casualties, their failure can lead to significant damage to surrounding structures, potential environmental contamination, and considerable economic ramifications from the loss of material and cost of replacement (Akbas and Uckan, 2014) – see Figure 2. Given the prevalance of storage silos throughout rural areas combined with their known vulnerability, an analysis of their structural behavior is imperative within the scope of rural resilience.

(a) (b) (c)

Figure 1. (a) Steel grain silos (photo by authors); (b) concrete grain silos (photo by authors) (c) above ground storage tank (photo by US Air Force: https://www.acc.af.mil/News/Photos/igphoto/2001731966/).

This paper is presented in two parts – the first dedicated to a digital/virtual reconnaissance of rural areas following natural hazards and the second dedicated to a more in-depth numerical analysis of the performance of steel storage silo structures. In the first part, reconnaissance data

is collected from various news outlets as well as weather and climate related government agencies (e.g., NOAA, NWS), in order to generate a preliminary understanding of rural resilience. The second part presents a numerical parametric study of the large grain silo structure. Previous efforts have focused on the wind pressure distribution on the general structure of the above ground storage tank with various roof systems including conical roof, flat roof, shallow conical, floating flat and dome roof (Portela and Godoy, 2004). In contrast, this paper will focus on those geometric configurations more closely related to the agricultural silos, which tend to be taller than above ground storage tanks. In this effort, a numerical model is developed in LS-DYNA and subsequently analyzed in a parametric study for various common geometric configurations. This paper presents the preliminary results of this study and outlines future research efforts to understand the behavior of these unique structures to extreme loads.

Figure 2. Three collapsed and severely damaged grain silos following Hurricane Harvey in Refugio, TX (photo courtesy of US Department of Agriculture: https://www.flickr.com/photos/usdagov/36508165554).

DIGITAL RECONNAISSANCE

Methodology

In order to evaluate and quantify the amount of hazard damage to rural communities around the United States and Canada, a digital (virtual) reconnaissance was conducted from January through August 2018. The digital reconnaissance process consisted of three distinct steps: 1) identifying the occurrence of a natural hazard in a rural community, 2) classifying the event by hazard type, and, 3) classifying by structural system damaged.

The National Oceanic and Atmospheric Administration (NOAA) damage survey viewer website as well as Google News were the two main sources used in order to identify rural hazard events (NOAA 2018). The data presented on the damage survey viewer interface is collected during National Weather Service (NWS) Post-Event Assessments and allows the user to search preliminary tornado and windstorm damage paths. The damage survey viewer's primary function is to compile and document high wind events and tornado tracks throughout the US, not to document rural damage. However, the site is particularly useful for indicating that a windstorm or tornadic event occurred, which could be studied for potential rural damage. The identification of an event from the damage survey viewer was then supplemented through a targeted search for media coverage of the event in local news outlets. Since not all hazard events are documented in the damage survey viewer, additional media searches were conducted using Google News as the primary search engine using keywords such as: *tornado*, *rural*, *farm*, *wind*, *damage*, *silo*, *grain bin*, *irrigation*, etc. The Google News component of the digital reconnaissance was particularly

useful as it searches a wide range of news sources, including very small community-based news outlets, which document damage that can severely impact a rural community but not be widespread enough to impact the national or even regional news. It is noted that the use of the NWS Damage Survey Viewer and Google News as the primary data sources is not comprehensive; however, the data collected can serve as a lower-bound for damage suffered by rural communities and can be indicative of areas of future need.

Once a hazard event was identified, it was first classified by type of hazard such as: 1) tornado, 2) straight-line wind, 3) thunderstorm, and, 4) other (e.g. earthquake). Due to the relatively low frequency of earthquake events with potential to cause damage combined with the relatively high frequency of wind-induced damage, the wind events were further classified and all other hazards were treated as a single group for statistical analysis. The final classification was with respect to the structure or other component damaged: 1) irrigation (e.g. center pivot) system, 2) crop, 3) agricultural equipment, 4) barn or agricultural structure, 5) bin or silo, 6) standard residential home, 7) manufactured/ and or mobile home damage, and, 8) unspecified rural damage, which included documentation of tree damage and instances when specifics regarding the damage were not included in the news coverage. Each of these classifications are shown photographically in Figure 3.

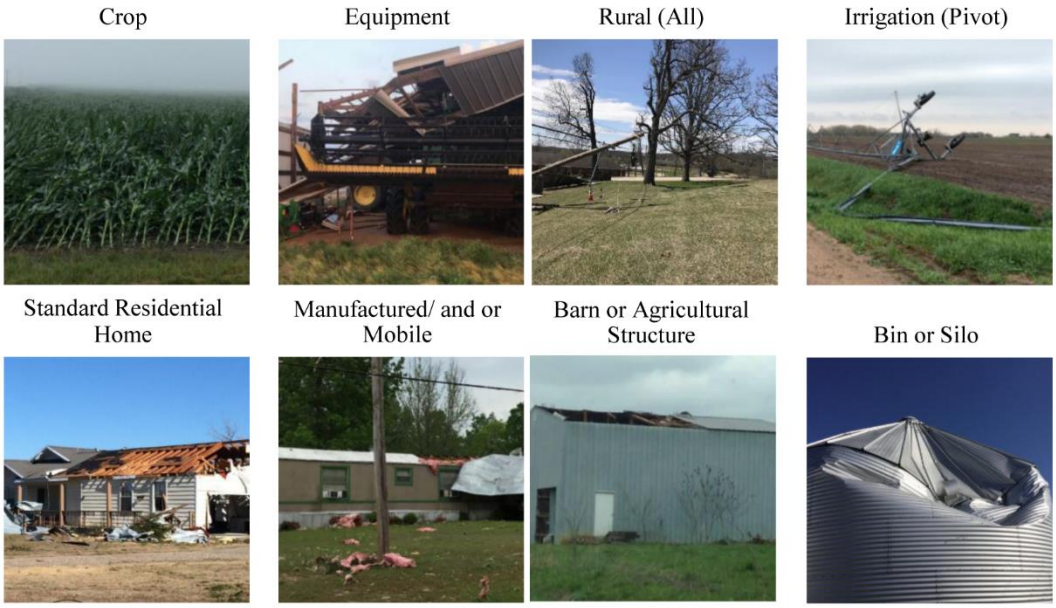

Figure 3. Classification of type of damage. Photos courtesy of National Oceanic and Atmospheric Administration.

Results and Discussion

The results of the digital reconnaissance were first analyzed in terms of geographic distribution to understand if the vulnerability of rural communities is more prevalent in certain geographic regions. While instances of rural earthquake damage were noted elsewhere in the world (e.g. Peru, Mexico), no damage-inducing earthquakes were observed in the United States or Canada during the time period of the digital reconnaissance (January – July 2018). Therefore, the geographic distribution presented in Figure 4 includes only wind events, including tornadoes, thunderstorm, and straight-line wind, that resulted in documented rural damage. In this map, the

damage source is indicated by the color of the marker. As seen in this map, a total of 181 damage-inducing events were collected including 173 in the United States and 8 in Canada over the seven-month duration of the digital reconnaissance. In total 31 of 50 states in the US and 4 of 13 provinces in Canada had rural communities impacted by a wind event. While this represents greater than 60% of the states in the country, it is clear from the map representation that it is concentrated east of the Rocky Mountains with no damage data along the west coast of the country. However, it is noted that western rural communities are still vulnerable to hazards; and, a cursory review of news coverage beyond the seven-month duration presented indicate damage in these areas. In addition, it is noted that evidence of wind-induced rural damage occurs in many other areas of the world, with significant coverage and documentation of rural communities in Australia and New Zealand.

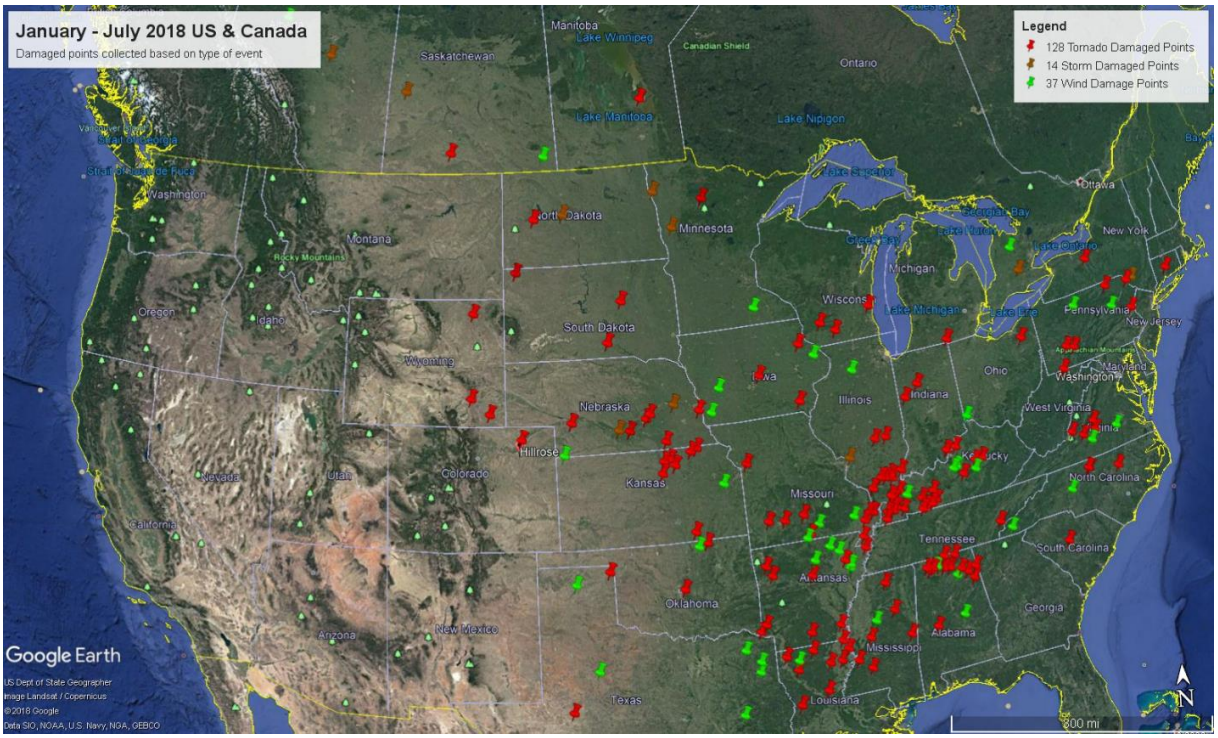

Figure 4. Rural resilience results based on type of damage

The digital reconnaissance was further analyzed by the type of damage observed, which is presented in bar chart form in Figure 5. The most prevalent type of damage documented was to residential housing, with a total of 160 events including 91 instances of damage to standard residential construction, 46 instances of damage to manufactured/mobile housing, and 23 instances of unspecified home damage. The most common damage documented for housing focused on the roof system, although detailed information regarding damage mechanisms is out of the scope of this digital reconnaissance. The second most common type of damage observed in the digital reconnaissance was to agricultural buildings including barns and storehouses, which accounted for 120 events and similarly included substantial documented roof damage but also included many instances of collapse. Following the documentation of building failures including both houses and agricultural structures, damage to grain silos, agricultural support equipment, crops, and irrigation systems accounted for 24, 18, 13, and 13 events, respectively. While the number of events that resulted damage to non-building structures were considerably

less than those resulting in building damage, this is not necessarily reflective of the structural vulnerability. Provided that the source for the type of damage was primarily news and media, the data collected likely contains significant bias towards housing or other large structures which impact a number of people. Despite the potential for bias, the digital reconnaissance highlights the remarkably high number of damage events that occurred over the relatively short duration of the study.

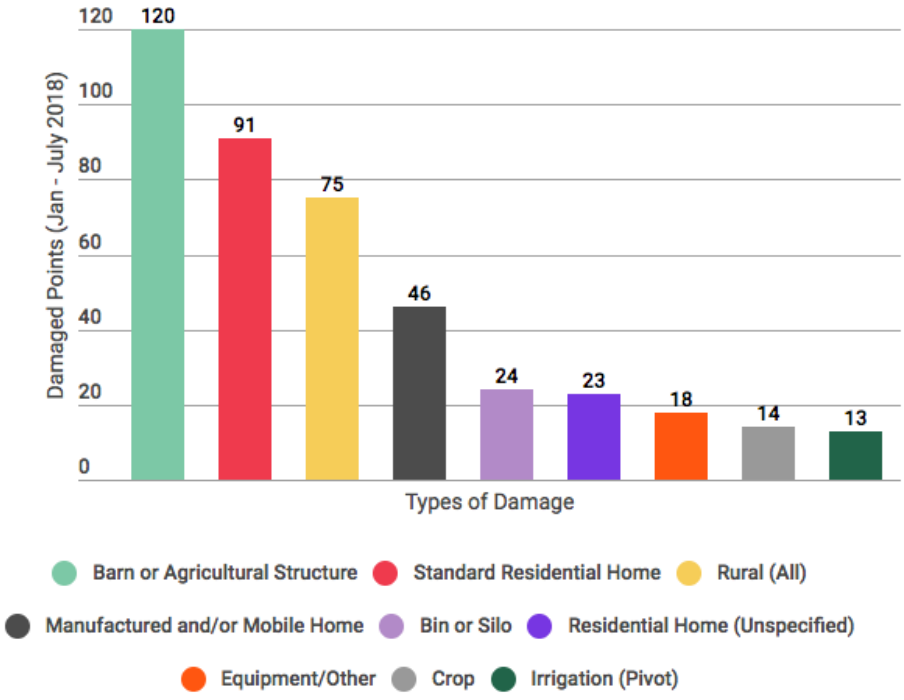

Figure 5. Rural resilience results based on structural system damaged

NUMERICAL MODELING: GRAIN SILOS

Model Development

In order to understand the response and vulnerability of a large grain silo structure subjected to high windstorms, a parametric study was carried out in order to identify vulnerable configurations and compare to the limited number of detailed reconnaissance observations. The multi-physics and finite element analysis platform, LS-DYNA, was used to carry out the analyses. The baseline geometry of the numerical model for the silo is shown in Figure 6 and was initially based on the geometry studied by Virella and Godoy (2003). This geometry was chosen since the wind pressure distribution was determined in the previous study via wind tunnel testing, the results of which could be used in the present numerical modeling and parametric study. While in reality the base of the silo can be freestanding or anchored, the base of the modeled silo was initially fixed. The steel material of the silo was modeled as elastic for the present analyses. The silo walls and roof were modeled using fully integrated shell elements – see Figure 7. The results of an eigenanalysis in LS-DYNA for the baseline model were compared with the natural periods presented by Virella and Godoy (2003) for preliminary validation of the

modeling strategy.

In order to gain preliminary understanding of the buckling behavior of the storage silos, wind pressure was applied as a static load to the silo. The wind pressure distribution was guided by the results of the wind tunnel testing of Portela and Godoy (2005), which was conducted for an above ground storage tank with a height-to-diameter ratio of approximately 0.43. The wind pressure distribution obtained in the previous study can be approximated by the function below, where θ indicates the circumferential location along the silo wall with respect to the windward meridian:

$$C_p = -0.2055 + 0.2943cos\theta + 0.4897cos2\theta + 0.2624cos3\theta - 0.0353cos4\theta \\ -0.0092cos5\theta + 0.0778cos6\theta + 0.0263cos7\theta \quad (1)$$

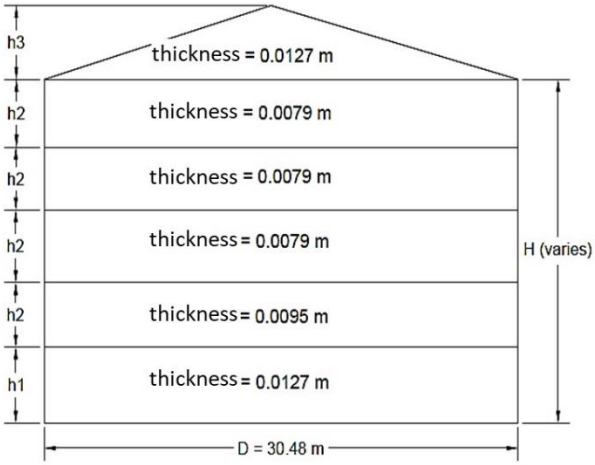

Figure 6. H = 19.337 m, 12.191 m, 7. 257 m; for H/D = 0.40, h1 = 2.425 m, h2 = 2.416 m, h3 = 2.858 m

Figure 7. Mesh of silo with aspect ratio *H*/*D* = 0.63 and 29,880 shell elements

For the parametric study, a total of twelve trials were performed with different variables. The first variable tested was the aspect ratio and geometry of the cylindrical shells. Eight trials were

conducted with four different aspect ratios: H/D = 0.24, H/D = 0.4, H/D = 0.63, and H/D = 1, for the first four the height was changed (Diameter = 30.48 m) and the following four the diameter was changed (Height = 19.337 m). For the last four trials the model with aspect ratio H/D = 0.63 was selected as a baseline. The second variable tested was the wall thickness of the cylindrical shell. For the first trial a 95% of the baseline thickness was analyzed and for the second trial a 105% of the baseline thickness was analyzed. The third and final variable tested was the slope of the roof. The first trial was analyzed with a flat roof and the second trial with a higher pitch roof compared to the baseline model. The total numbers of elements in the finite element mesh for the silo models are listed in Table 1. For each model developed, a linear buckling analysis was performed in order to gain a preliminary understanding of how the silo structure would fail and at what magnitude of wind pressure. It is recognized that a linear buckling analysis overestimates the buckling load and yields nonconservative results. However, the analyses presented are intended to guide further research and not provide definitive conclusions regarding storage silo performance.

Table 1. Total number of elements for the finite element meshes of the tank models

H/D	Changed Height (D = 30.48 m)	Changed Diameter (H = 19.337 m)	High Pitch Roof	Flat Roof
0.24	25084	53462		
0.4	26812	67188		
0.63	29880	29937	31188	29456
1	33884	13878		

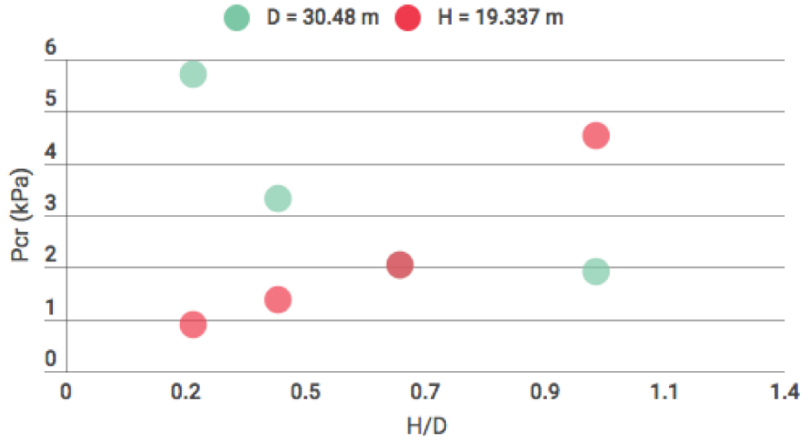

Figure 8. Aspect ratio and geometry of cylindrical shells

Results of Parametric Study

The results for the first variable tested, the aspect ratio and geometry of the steel storage silo, are presented in Figure 8. This scatter plot indicates the value of the critical buckling load, P_{cr}, as a function of the silo aspect ratio (defined in Figure 6). The dimension that was consistent throughout the parametric study is indicated by the color in the scatter plot, where green indicates a consistent diameter of 30.48 m and red indicates a consistent height of 19.337 m. It can be seen that the aspect ratio of a grain silo structure substantially influences the buckling load on the cylindrical wall with variations on the order of hundreds of percent. It is shown that as the height increases and the diameter stays constant, the buckling capacity decreases. As the

diameter increases and the height stays constant, the buckling capacity increases. Despite the significant variation in terms of the critical buckling load for the geometry, the buckling mode shape dominantly stayed the same with buckling primarily localized to the windward cylindrical wall – see Figure 9. In addition to the geometric variations, the wall thickness and roof slope were significant variables in the critical buckling load. Specifically, the critical pressure for the 95% wall thickness model was 1.81 kPa compared to 2.33 kPa for the 105% wall thickness model. This is a logical trend, yet it lends credence to further studies of the impact of rust and material loss as well as material imperfections. Similarly for the roof slope, variations in terms of the critical buckling load were observed, but were noticeably smaller than the variations observed due to geometry. Specifically, the critical pressure for the flat roof pitch was 1.24 kPa and for the higher roof pitch, 2.068 kPa.

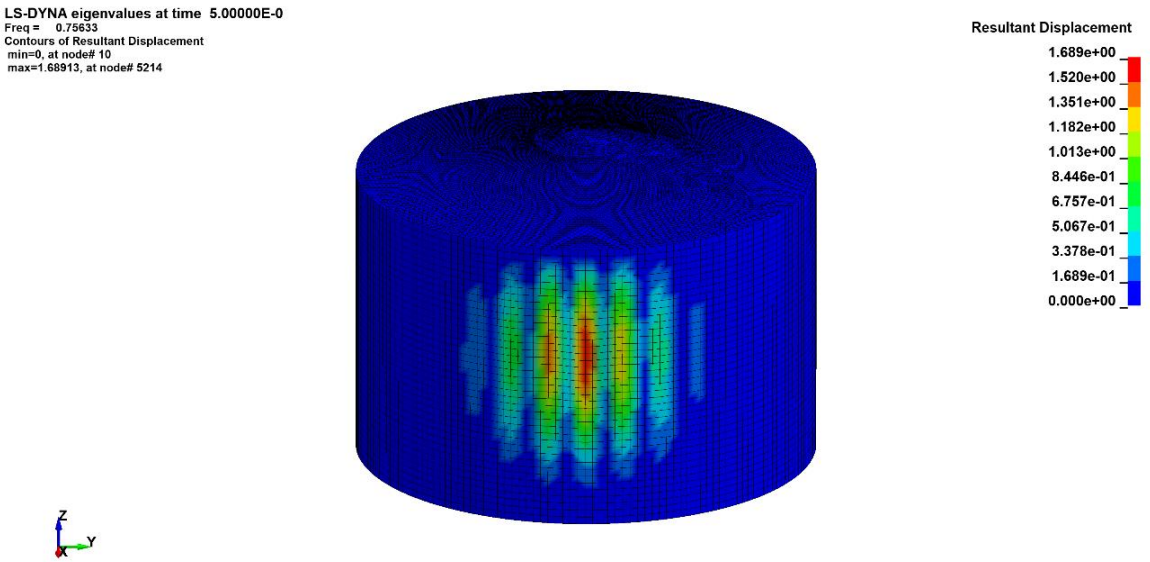

Figure 9. First buckling mode shape for the baseline storage silo.

CONCLUSIONS AND FUTURE WORK

The results presented for the digital reconnaissance study over a seven-month period *emphasize significant damage to a wide range of rural systems* during relatively modest events across many different states and countries for multiple hazard types. The numerical study indicates that grain bins with self-supported roofs are likely to sustain damage to the cylindrical portion of the structure. Furthermore, the geometry of the cylinder and the wall thickness are significant factors in the performance of steel grain silos during high wind events.

Future studies will investigate the impact of anchorage mechanisms, roof support systems, and geometric and material imperfections on the performance of steel grain silos to both wind and other natural hazards. As a result of the digital reconnaissance, significant effort will also be directed towards other critical agricultural systems including warehouse type buildings and irrigation systems.

ACKNOWLEDGEMENTS

Over the course of this research, the first author was supported by the National Science Foundation Research Experience for Undergraduates (REU) site program, Sustainability of

Horizontal Civil Networks in Rural Areas, at the University of Nebraska-Lincoln. The authors also acknowledge the support of the University of Nebraska-Lincoln's Summer Research Program. This work was completed utilizing the Holland Computing Center of the University of Nebraska, which receives support from the Nebraska Research Initiative.

REFERENCES

Akbas, B., & Uckan, E. (2012). *Seismic and structural observations from Van earthquakes of October 23 and November 9, 2011. Gebze Institute of Technology, Department of Earthquake and Structural Engineering* (No. 2012/01, p. 1). Report.

Bloch, A. (2018, January 4th). 2017's natural disasters cost American agriculture over $5 billion. *The new food economy*. Retrieved from https://newfoodeconomy.org

Cutter, S. L., Ash, K. D., & Emrich, C. T. (2016). Urban–rural differences in disaster resilience. *Annals of the American Association of Geographers*, *106*(6), 1236–1252.

Dogangun, A., Karaca, Z., Durmus, A., & Sezen, H. (2009). Cause of damage and failures in silo structures. *Journal of performance of constructed facilities*, *23*(2), 65–71.

Kameshwar, S., & Padgett, J. E. (2018). Fragility and Resilience Indicators for Portfolio of Oil Storage Tanks Subjected to Hurricanes. *Journal of Infrastructure Systems*, *24*(2), 04018003.

Li, H. (1994). "Analysis of steel silo structures on discrete supports." Ph. D. thesis, Univ. of Edinburgh, Edinburgh, Scotland, U.K.

Making further supplemental appropriations for the fiscal year ending September 30, 2018, for disaster assistance for Hurricanes Harvey, Irma, and Maria, and calendar year 2017 wildfires, and for other purposes, H.R. 4667, 115th Cong. (2017).

National Research Council (NRC). (2012). *Disaster resilience: A national imperative*. Washington, DC: National Academic Press.

National Oceanic and Atmospheric Administration (NOAA). (2017). Damage Assessment Toolkit. https://apps.dat.noaa.gov/stormdamage/damageviewer/

New Census Data Show Difference Between Urban and Rural Populations (2016, December 8th), *Census Newsroom*. Retrieved from https://census.gov

Portela, G., & Godoy, L. A. (2005). Wind pressures and buckling of cylindrical steel tanks with a conical roof. *Journal of Constructional Steel Research*, *61*(6), 786–807.

Virella, J. C., Godoy, L. A., & Suárez, L. E. (2003). Influence of the roof on the natural periods of empty steel tanks. *Engineering Structures*, *25*(7), 877–887.